Please cite this article in press as: Ito et al., Systematic Analysis of Neural Projections Reveals Clonal Composition of the *Drosophila* Brain, Current Biology (2013), http://dx.doi.org/10.1016/j.cub.2013.03.015

Current Biology *23*, 1–12, April 22, 2013 ©2013 Elsevier Ltd All rights reserved http://dx.doi.org/10.1016/j.cub.2013.03.015

Article

Systematic Analysis of Neural Projections Reveals Clonal Composition of the *Drosophila* Brain

Masayoshi Ito,[1,2] Naoki Masuda,[3] Kazunori Shinomiya,[1,4] Keita Endo,[1,5] and Kei Ito[1,2,*]

[1]Institute of Molecular and Cellular Biosciences (IMCB), The University of Tokyo, 1-1-1 Yayoi, Bunkyo-ku, Tokyo 113-0032, Japan

[2]Graduate School of Arts and Sciences, The University of Tokyo, 3-8-1 Komaba, Meguro-ku, Tokyo 153-8902, Japan

[3]Department of Mathematical Informatics, The University of Tokyo, 7-3-1 Hongo, Bunkyo-ku, Tokyo 113-8656, Japan

Summary

Background: During development neurons are generated by sequential divisions of neural stem cells, or neuroblasts. In the insect brain progeny of certain stem cells form lineage-specific sets of projections that arborize in distinct brain regions, called clonal units. Though this raises the possibility that the entire neural network in the brain might be organized in a clone-dependent fashion, only a small portion of clones has been identified.

Results: Using *Drosophila melanogaster*, we randomly labeled one of about 100 stem cells at the beginning of the larval stage, analyzed the projection patterns of their progeny in the adult, and identified 96 clonal units in the central part of the fly brain, the cerebrum. Neurons of all the clones arborize in distinct regions of the brain, though many clones feature heterogeneous groups of neurons in terms of their projection patterns and neurotransmitters. Arborizations of clones overlap preferentially to form several groups of closely associated clones. Fascicles and commissures were all made by unique sets of clones. Whereas well-investigated brain regions such as the mushroom body and central complex consist of relatively small numbers of clones and are specifically connected with a limited number of neuropils, seemingly disorganized neuropils surrounding them are composed by a much larger number of clones and have extensive specific connections with many other neuropils.

Conclusions: Our study showed that the insect brain is formed by a composition of cell-lineage-dependent modules. Clonal analysis reveals organized architecture even in those neuropils without obvious structural landmarks.

Introduction

Neural computation in the brain is accomplished by its complex neural network. A broad and detailed knowledge of neural projection patterns is a prerequisite to understanding how such networks are organized [1]. During development, a neural stem cell divides asymmetrically to give birth to a family of clonally associated neurons [2, 3]. Growing evidence, both from vertebrate and invertebrate brains, suggests the importance of clonal organization in the network formation and function. In the mammalian brain, sibling neurons of the same lineage tend to have more synaptic contacts with each other, suggesting closer functional association [4]. Clonally related neurons can share characteristic functions, such as those in the visual cortex that detect similar visual features [5, 6].

Neurons of the insect brain are also formed by the stem cells, called neuroblasts. Progeny of certain neuroblasts compose specific brain components such as the antennal lobe (AL), the mushroom body (MB), and the central complex (CX) [7–10]. The set of clonally related neurons and their specific arborizations is called a clonal unit [7, 10], which serves as the building block that constructs the neural network of at least some of the brain's neuropils.

The *Drosophila melanogaster* brain consists of about 100,000 neurons, and its central part, called the cerebrum (which excludes the optic lobe and the subesophageal ganglion (SEG) is estimated to have about 15,000 neurons each side of the midline (data not shown). These cerebral neurons are generated by about 100 neuroblasts during development [11, 12]. Most neuroblasts, except for the four MB neuroblasts and one lateral AL neuroblast, have two phases of proliferation during early to midembryonic and early larval to early pupal stages, producing neurons of the primary and secondary lineages, respectively [11, 13]. Neuroblasts are classified as type I and II. Most neuroblasts are type I; their daughter cells, called the ganglion mother cells (GMCs), divide once again to give birth to two neurons each. In contrast, eight type-II neuroblasts give birth to intermediate neural progeny, which divide several times to generate a larger number and more varieties of neurons [14, 15].

In spite of extensive studies performed so far [7–12], including the clonal analysis of diverse *fruitless*-expressing neurons [16, 17], several key questions remain unanswered. Given the number of neuroblasts, as many as 100 clonal units should exist in the adult brain. Do they all feature specific arborizations that contribute to distinct brain components? Is each clone unique? How do neurons of different lineages overlap to form a closely associated functional group called the clan [10]? Are the neurons of a clone structurally and biochemically uniform or diverse? To answer these questions, we performed a large-scale analysis for the thorough identification of clonal structures.

In spite of the recent advances in the systematic single-neuron-labeling and multicolor cell-labeling methods such as Brainbow [18, 19], complete identification of tens of thousands of neurons is not technically easy. Comprehensive analysis of the much fewer number of clonal units, the combination of which should contain the entire neural projection patterns, provides a systematic overview of the brain-wide neural network efficiently. It also gives indispensable insights for understanding how complex brain architecture is developmentally and evolutionarily organized.

[4]Present address: Department of Psychology and Neuroscience, Dalhousie University, 1355 Oxford Street, Halifax, NS B3H 4R2, Canada

[5]Present address: RIKEN Brain Science Institute, 2-1 Hirosawa, Wako, Saitama 351-0198, Japan

*Correspondence: itokei@iam.u-tokyo.ac.jp

Please cite this article in press as: Ito et al., Systematic Analysis of Neural Projections Reveals Clonal Composition of the *Drosophila* Brain, Current Biology (2013), http://dx.doi.org/10.1016/j.cub.2013.03.015

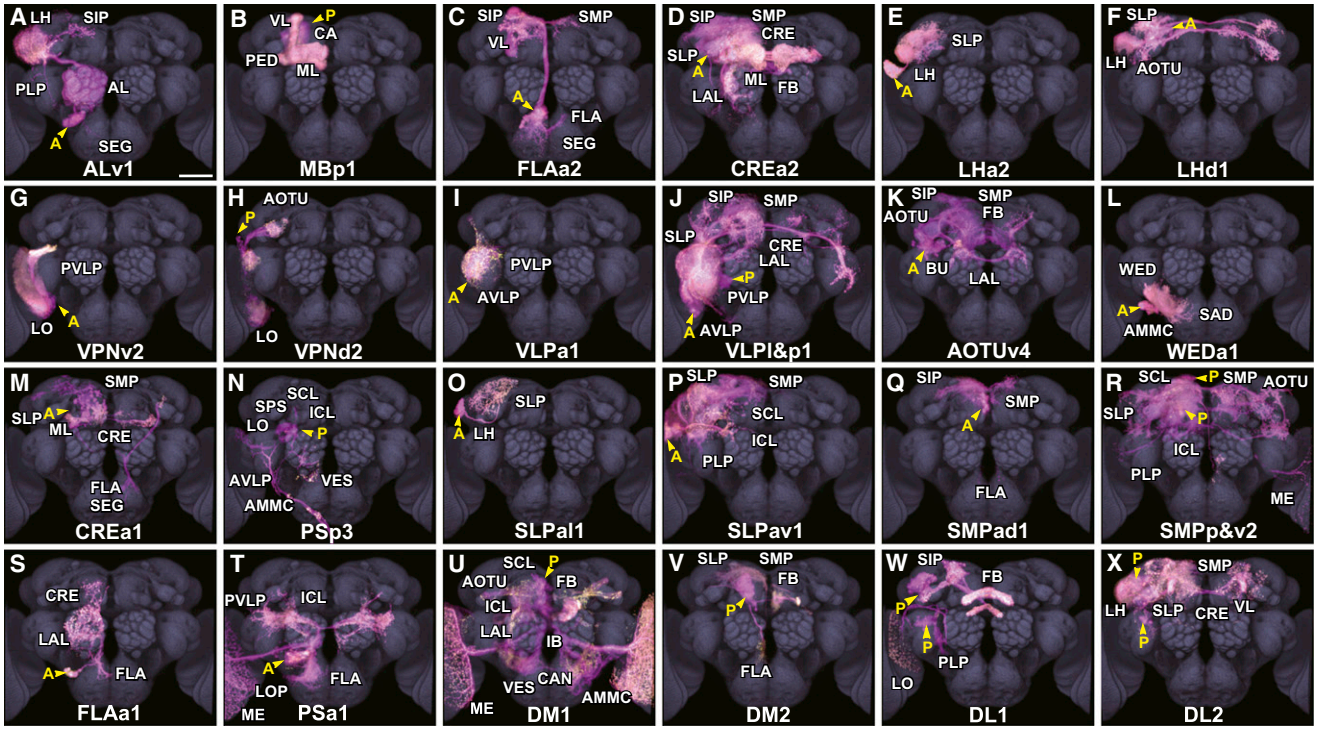

Figure 1. Examples of Clonal Units in the Adult *Drosophila* Brain

Anterior view of 3D reconstructions. Cell bodies and neuronal fibers (magenta), distributions of presynaptic sites (white), and the entire neuropil of the template brain (gray) are shown. Arrowheads indicate the location of cell-body clusters, with the letters "A" and "P" denoting their positions in the anterior or posterior brain, respectively. Images of the entire set of the identified clones are shown in Figure S1. See Table S2A for the names of neuropils. Scale bar represents 50 μm. Genotypes: *elav^{c155}-Gal4 hs-FLP/UAS-DsRed*; *FRT^{G13} tub-GAL80/FRT^{G13}*; *UAS-nSyb::GFP, elav^{c155}-Gal4 hs-FLP/UAS-Syt::HA*; *FRT^{G13} tub-GAL80/FRT^{G13} UAS-GFP*; *UAS-mCD8::GFP/+, hs-FLP tub-GAL80 FRT^{19A}/UAS-DsRed FRT^{19A}*; *actin-Gal4/ +*; *UAS-n-Syb::GFP/+*.

Results

Visualization of Cell Lineage-Dependent Clonal Units in the Adult *Drosophila* Brain

To visualize clonal units, we labeled the progeny of single neuroblasts, using the mosaic analysis with a repressible cell marker (MARCM) technique [20]. We used actin-GAL4 or elav-GAL4 to drive expression in all the neurons and induced flippase-mediated chromosomal recombination with mild heat shock in late embryos or early first-instar larvae to label all the neurons of the secondary lineages. To estimate the direction of information in the labeled neurons, we visualized neural fibers and presynaptic sites using combinations of cytoplasmic reporters (DsRed or GFP) and synaptic vesicle-targeted fusion reporters (neuronal synaptobrevin [n-Syb]::GFP or synaptotagmin [Syt]::HA). Considering the potential cell-specific variability in the labeling intensity and flipping frequency, we used various combinations of drivers, reporters, and locations of recombination targets to reveal a wider variety of clones.

We analyzed in total about 5,000 brain samples, and the labeled clones that share locations of cell bodies and characteristic projection patterns were classified (Figure 1). We sometimes found clone samples that visualize characteristic subsets of arborizations observed in other samples. Given that this could happen either because flippase-mediated recombination would have occurred later during development or because of the variety of expression-driver activity among cells, we determined that these samples were labeling the same clone.

We identified 80 groups of neuroblast clones with a single cluster of cell bodies. In addition, we found 14 groups of cells that feature two or three clusters of cell bodies in different parts of the brain. Because these clusters are colabeled reproducibly in all the samples examined, including those in the companion study by Yu et al. in this issue of *Current Biology* [21], it is highly likely that the labeled neurons belong to a single neuroblast clone despite their distant locations. Most of the two-cell clones, labeled by the flippase activity in the GMCs, showed projection patterns that are subsets of the above clones. However, we found two notable exceptions whose arborization patterns do not match with any of the above. Because their lineage identity is not yet resolved, we treated them as visualizing projections of potentially distinct neuroblast clones (see Supplemental Discussion available online). Thus, we identified in total 96 clonal units (94 clearly identified and two potential clones) (Figure S1 and Table S1). Three-dimensional (3D) confocal serial section data of the clones are available via the FLYBRAIN Neuron Database (http://ndb.flybrain.org).

The 3D data of the clones acquired from different samples were put into a standard template [16], using linear and nonlinear registration methods [22, 23], and overlaid for comparison (Figure 3A; Movie S1). Arborizations of the clones together covered nearly the entire volume of the cerebrum. The opposite hemisphere was also covered extensively, because 51 of the identified clones project also to the contralateral brain. The ventralmost part of the cerebrum was covered less extensively, because the current study

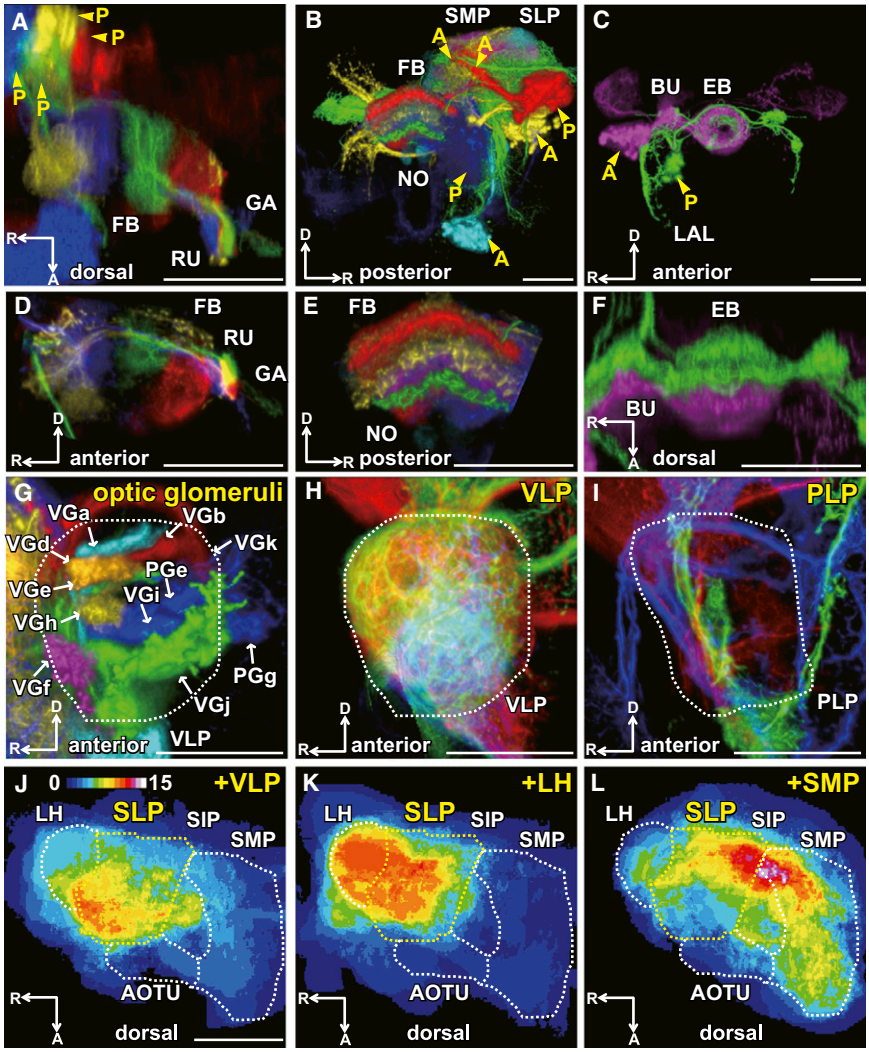

Figure 2. Clonally Organized Structures in the Brain

Three-dimensional reconstruction of selective clones viewed from the directions indicated in each panel.

(A–F) Clones of the central complex (CX). Those deriving from one side of brain are shown. Clones that contain small-field neurons of the CX are shown in (A). Clones containing large-field CX neurons are shown in (B). Two clones that preferentially project to the ellipsoid body (EB) are shown in (C). (D) is an anterior close-up view of (A), showing the output terminals in the rubus (RB) and gall (GA) with overlapping projections from the four clones. (E) is a posterior close-up view of (B), showing six discrete layers of clonal arborizations in the fan-shaped body (FB). (F) is an anterior-dorsal close-up view of (C), showing anteroposterior layers in the EB.

(G) Terminals of the VPN clones in the VLP and PLP, seen in different colors. Arrows indicate the optic glomeruli.

(H and I) Close-up views of the VLP and PLP, showing characteristic arborization patterns of the cerebral clonal units. Clones shown in the overlay are DM1, DM2, DM3, and DM4 (A and D); DM6, DL1, AOTUv4, CREa2, LALv1, and SMPad4 (B and E); EBa1 and EBp1 (C and F); VPNd1, VPNd3, VPNp2, VPNp3, VPNv1, VPNv2, and VPNv3 (G); VLPl2, VLPl&p1, and VLPl&p2 (H); and SLPp&v1, WEDa2, and SLPa&l1 (I).

(J–L) Horizontal cross-section view of the dorsal brain, showing the overlay of arborizations of the clones associated with the SLP (indicated with yellow dotted lines) and neighboring neuropils. Color code in (J) denotes the degree of clonal overlap. See also Figure S2. A, anterior; R, right; D, dorsal (body axis). Scale bar represents 50 μm.

excluded the clones of the SEG, many of which arborize in this region.

To document the arborization patterns of the identified clones (Tables S2 and S3), we used the systematic nomenclature system of the entire fly brain proposed by the Insect Brain Name Working Group (Insect Brain Name Working Group, unpublished data), which separates the brain into 44 regions (neuropils) per side (Table S2A). Arborizations of a distinct part of 36 clones matched well with the proposed neuropil boundaries (Figures S2A–S2H and Table S2B). Arborizations that cross these boundaries were also observed often, but when arborizations of multiple clones were overlaid, they tended to show correlation with certain boundaries (Figures 2J–2L; Figures S2I–S2N).

We developed a unified naming scheme of the clonal units in collaboration with the Yu et al. companion study [21], so that identical clones should have the same name. Clones are named using three designators: neuropil, cell body location, and number. They were first categorized according to the associated neuropils. Because many clones innervate multiple neuropils, we took the neuropil where the neurites emerging from the cell bodies form the first arborizations or in which the clone arborizes most prominently. The clones were subsequently categorized according to the location of the cell-body clusters (anterior, posterior, lateral, dorsal, or ventral, in body axis). For the clones with multiple cell-body clusters, two characters were added to indicate their relative locations.

Clones in each subcategory were numbered according either to the simplicity or to the fine location of cell-body clusters. Number was added even when there was only one clone type in the subcategory, so that other clones that might be identified in the future can easily be distinguished. Six of the clones that derive from the eight PAN (posterior asense-negative) cell lineages [21] were named DM1-6 to keep consistency with previous studies [24]. The remaining two PAN clones were named DL1 and DL2 because of their dorsolateral locations.

Clonally Composed Architecture in the Brain

Identified clones showed strong correlation with the functional architecture of the brain (Figure 1). We first found clear association between clonal units and sensory pathways. As reported previously [7, 9], the clones associated with the AL and MB—the primary and major secondary olfactory centers—are formed by specific clones (Figures 1A and 1B). Higher olfactory pathways are also formed by distinct clones. The associative lobe regions of the MB are innervated by specific clones that contain MB-extrinsic neurons [25] (Figures 1C and 1D), and the other major secondary olfactory center—the lateral horn (LH)—is contributed by clones that either arborize locally (Figure 1E) or send projections to other neuropils (Figure 1F).

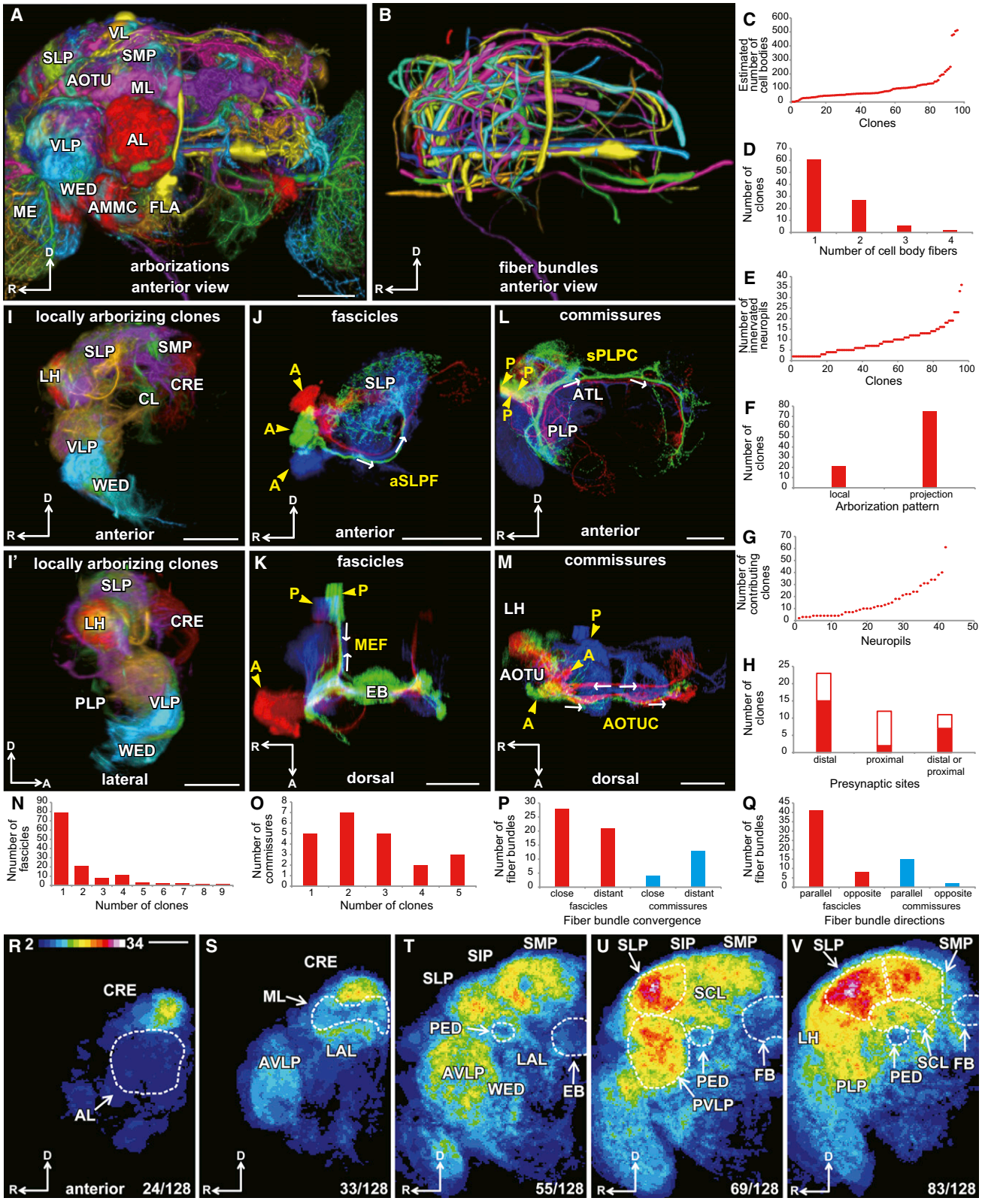

Figure 3. Spatial Associations of the Identified Clones

(A) Overlay of all the identified clones, anterior view. Signals of cell bodies are removed to visualize the underlying neural projections. See also Movie S1.

(B) Distribution of the identified neuronal fiber bundles, anterior view.

(C–H) Quantitative characterization of clonal attributes. For (H), red bars indicate the number of clones that exclusively contain projections with asymmetric distribution of presynaptic sites, and white bars indicate the number of clones that contain mixed projections with either symmetric or asymmetric distribution of presynaptic sites. The rightmost bar indicates the number of clones that contain mixed projections with presynaptic sites either in their distal or proximal parts. See also Figure S3.

(legend continued on next page)

The visual pathways are also formed by distinct clonal units. Each pathway of the visual projection neurons (VPNs) [26], from the primary visual center in the optic lobe to the secondary visual centers in the cerebrum, is formed by distinct clones (Figures 1G and 1H). One of the secondary visual centers, the posterior ventrolateral protocerebrum (PVLP; see Table S2A for abbreviations of neuropils), is also contributed by distinct clones that either arborize locally (Figure 1I) or project to other neuropils (Figure 1J). Another secondary visual center, the anterior optic tubercle (AOTU), is contributed by specific VPN clones (Figure 1H) and clones connecting the AOTU with distinct neuropils in the cerebrum (Figure 1K), forming a clonally organized visual pathway from the optic lobe via the AOTU to higher visual centers. We also found several clones that arborize in the auditory (Figure 1L) and gustatory (Figure 1M) primary centers [27, 28]. The motor pathway is also associated with clones; the descending neurons we identified derive from three distinct clones (Figure 1N).

In addition to these clones, we found 38 clones that arborize preferentially in other neuropils than the known sensory or motor centers. For example, the superior lateral protocerebrum (SLP) and superior medial protocerebrum (SMP) are contributed by clones that arborize locally (Figures 1O and 1Q) or in multiple neuropils connected via projections (Figures 1P and 1R). Such clones are also observed in the more ventral parts of the cerebrum (Figures 1S and 1T). The eight PAN clones also belong to this category (Figures 1U–1X), sending projections to many brain regions, including the CX.

The CX is composed of three major types of clones. Four clones in the posterior brain provide so-called small-field neurons [29] (Figure 2A), whereas six clones in the anterior and posterior brain give rise to large-field neurons of the fan-shaped body (FB, Figure 2B). In addition, large-field neurons of the ellipsoid body (EB) are formed by two clones in the anterior and posterior brain (Figure 2C). Fine structures of the CX are also organized clonally. The small-field neurons of the four clones arborize in largely segregated areas of the FB but converge to form overlapping output sites in the regions of the anterior brain that are named rubus and gall by the Insect Brain Name Working Group (Insect Brain Name Working Group, unpublished data). (Figure 2D). Tangential arborizations of large-field neurons are known to have layered organization, each of which may have different functions [30]. We found that these layers are clonally organized, with each clone contributing to specific layers (Figure 2E). The ring structure of the EB also has anterior and posterior segregation formed preferentially by the anterior and posterior clones, respectively (Figure 2F).

Because of the relatively homogeneous appearance when visualized with classic labeling methods, brain regions other than the AL, MB, and CX are often collectively referred to as "diffuse neuropils," whose structure and functions have hardly been investigated so far. The identified clonal units feature clearly organized projections also in these neuropils.

The clonal VPNs arising from the optic lobe form bulbous masses of terminals called the optic glomeruli [26, 31]. Optic glomeruli are therefore clonally constructed structures (Figure 2G). The ventrolateral protocerebrum (VLP, combination of anterior ventrolateral protocerebrum [AVLP] and PVLP) and posterior lateral protocerebrum (PLP), which houses these optic glomeruli, appear similar when examined with conventional silver stain or synaptic labeling with nc82 antibodies. However, they are very different when we compare the architecture of the non-VPN clones arborizing in these regions. These clones tend to have broad and overlapping projections in the VLP (Figure 2H) but arborize in small discrete domains in the PLP (Figure 2I). In addition, the VLP has many clones that arborize locally in the neuropil, whereas the PLP is devoid of such local clones (Figure 3I).

Clonal units tend to form broad and overlapping arborizations in the dorsal brain region around the MB and CX, such as the SLP, SMP, superior clamp (SCL), and inferior clamp (ICL). Clone-dependent organization also exists in these neuropils. In the SLP, when arborizations of the clonal units that also innervate the neighboring VLP, LH, and SMP are overlaid separately, they have preferential arborizations in its anterior, middle, and posterior subregions, respectively (Figures 2J–2L). Likewise, clones associated with the AOTU and crepine (CRE) arborize in the anterior SMP, whereas those associated with the SCL and ICL arborize in its posterior part (Figures S2I–S2K). In the SCL and ICL, clones associated with the VLP, SLP, and PLP arborize in their anterior, middle, and posterior volumes, respectively (Figures S2L–S2N). Thus, subregions of these diffuse neuropils have preferential connections with specific other neuropils.

Structural Feature of the Clonal Units

From these data we were able to deduce several common characteristics of the clonal units. First, cell bodies of all the clones form one or a few tightly packed clusters in the cell-body rind (also called the cortex). The number of cells per clone is rather varied (Figure 3C), suggesting dynamic regulation of mitosis and apoptosis during development.

Second, all the neural fibers arising from a cell-body cluster form one or a few tight bundles (Figure 3D). Different bundles tend to project differently, and neurons projecting via the same initial bundle may further segregate to innervate different neuropils. Considering these, at least 60% of clones contain a heterogeneous population of neurons in terms of their arborization patterns.

Third, a clonal unit arborizes within distinct parts of the brain (Figure 3E). The complexity of innervation pattern varies considerably. About 40% of the clones arborize in up to five neuropils, whereas about 10% arborize in more than 15, some in as many as 36 neuropils. Not only clones deriving

(I) Distribution of the clones with locally confined arborizations within a single neuropil or neighboring neuropils. Anterior (I) and lateral (I′) views of the arborizations are shown.

(J–M) Fiber bundles formed by multiple clones. Three clones that contribute to a bundle are shown in different colors. Arrowheads indicate the cell-body clusters. Arrows indicate directions of fiber bundles from proximal to distal (from the cell bodies) parts of neurites. aSLPF, anterior SLP fascicle; MEF, medial equatorial fascicle; sPLPC, superior PLP commissure; AOTUC, AOTU commissure. Clones shown in the overlay: SLPpl4, SLPal1, and SLPal 2 (J); AOTUv3, EBp1, and DM5 (K); SLPp&v1, LHp2, and VPNp&v1 (L); LHd1, AOTUv2, and SMPp&v1 (M).

(N–Q) Quantitative characterization of fiber bundles.

(R–V) Number of clones contributing to neuropils. Frontal sections of the cerebrum (from anterior to posterior) show the color-coded number of clones that arborize in each small region of the brain. Color code is shown at the top margin of (R). White dotted lines indicate neuropils with high or low clonal overlap. Bottom right numbers denote the number of sections counted from the anterior. ML and PED are parts of the MB, and EB and FB are parts of the CX. A, anterior; R, right; D, dorsal (body axis). Scale bar represents 50 μm.

from type-II neuroblasts (e.g., Figures 1U and 1X) but also several clones made by type-I neuroblasts form complex projections (e.g., Figures 1J, 1R, and 1T). We found no clear correlation between the complexity of arborizations and the number of cells in the clone. Left/right asymmetry was not observed at the current resolution of clonal comparison.

Lastly, about 80% of clones (Figure 3F) feature multiple arborization sites that are connected with the axons of projection neurons (e.g., Figures 1A, 1C, 1F, 1J, 1P, 1R, and 1T). Other clones form single arborizations of local neurons that are either limited within a single neuropil or extend across a few neighboring neuropils (e.g., Figures 1E, 1I, and 1O). Interestingly, these locally arborizing clones were found preferentially in the anterior ventrolateral and posterior dorsal parts of the cerebrum (Figure 3I).

Number of Clones Contributing to Distinct Neuropils

Because of the spatial overlap between clones, each neuropil is contributed to by multiple clonal units. Whereas some neuropils receive contributions from less than 10 clones, a few neuropils are contributed by abundant clones, some as many as 61 (Figure 3G; Table S2B). The number of clones contributing to a particular neuropil may not directly indicate actual overlap, however, because some clones may arborize in its nonoverlapping subregions. For a more precise analysis, we divided the brain into small cuboids (voxels) and calculated the number of clones that arborize within each (Figures 3R–3V) (size of the voxel = 1.2 × 1.2 × 1.5 μm). Neuropils of the AL, MB, and CX appear dark in the color-coded section images, showing that voxels in these regions are contributed by significantly fewer clones—at the utmost, eight clones per voxel—than those in the surrounding diffuse neuropils like the SLP, SMP, PVLP, and SCL.

Correlation between Clonal Units and Neural Fiber Bundles

Different parts of the brain are connected by many fiber bundles. We therefore analyzed how they are correlated with clonal composition. We identified in total 150 fiber bundles (Figure 3B; Tables S2A and S2C), among which 128 connect ipsilateral parts of the brain (called fascicles, Figures 3J and 3K) and 22 connect bilateral neuropils (called commissures, Figures 3L and 3M). All the bundles are formed either by single or unique sets of a few clones (Figures 3N and 3O), indicating that the composition of fiber bundles is tightly associated with clonal units. Commissures tend to consist of more clones than fascicles: 38% of fascicles and 77% of commissures are contributed by multiple clones of the same side and, because we found no apparent left/right asymmetry concerning clonal structures, each commissure is likely to be contributed by the same number of clones of both sides.

During development, clonally related neurons send fiber bundles into neuropils. For the bundles contributed by multiple clones, fibers arising from different clones may converge right after they emerge out of the cell-body clusters (Figures 3J and 3L), or they may run a certain distance through the neuropils before they merge (Figures 3K and 3M). Both cases occur at about the same rate for the 49 fascicles with multiple clones (Figure 3P). For the 17 multiclone commissures, on the contrary, bundles of 76% of clones converge only when they have extended deep in the neuropil.

Neural fibers have a structural polarity from the cell body to the distal ends of neurites. When fibers from different clones converge during development, they may project either in the same (Figures 3J and 3L) or in opposite directions (Figures 3K and 3M). Of fascicles 84% and of commissures 88% within the hemisphere contain parallel fibers running in the same direction (Figure 3Q). Thus, developmentally, it is much more common that fibers deriving from different clones form parallel rather than opposite-running bundles.

Neural fibers also have functional polarity in terms of the direction of signal propagation. We found 46 clones in which at least some of their projections show clear asymmetric distribution of presynaptic sites (Figures S3A–S3C). It is often believed that the arborizations proximal to the cell bodies are dendritic. However, 23 out of the 46 clones contain projections with presynaptic sites only in their proximal arborizations (Figure 3H), indicating clear directional flow from the farther ends of these neurites.

Spatial Overlap between Clonal Units and Segmental Composition of the Brain

In order to communicate with neurons of other clones, arborizations of different clones must overlap [10]. Although spatial overlap does not directly indicate the presence of synaptic connections, clones whose arborizations overlap extensively should have a tighter functional relationship than those that hardly do. Cluster analysis based on the "distance" between all the combinations of clones, by calculating the degree of overlap between them, revealed that the clones could be classified into four groups (Figure 4A). Three clone groups arborize primarily in the dorsal-lateral, dorsal-medial, and ventral regions of the cerebrum, respectively, and the fourth group consists of the visual projection neurons that share large arborizations in the optic lobe (Figures 4B–4E).

Developmentally and evolutionarily, the insect cerebrum consists of three neuromeres: the proto-, deuto- and tritocerebra [32]. During neurogenesis, neural fibers deriving from each neuromere merge extensively, making the identification, in the adult, of neuromere boundaries extremely difficult. We expected that the boundaries might be resolved by analyzing the spatial overlap of clones that belong to each neuromere. Contrary to our expectation, putative deuto- and tritocerebral clones, whose cell bodies lie at the level ventral (developmentally more posterior) to the AL, did not form distinct overlap clusters but were split into three above-mentioned major clusters together with protocerebral clones (Figures 4B–4D). Cluster analysis specifically of these putative deuto- and tritocerebral clones did not reveal neuromere organizations either (Figure 4F; Figure S4). These data suggest that much of the adult brain composition may be unrelated to its segmental origin.

Biochemical Heterogeneity within Clonal Units

Complex computation by neural networks involves nerve cells with diverse physiological functions, such as excitatory and inhibitory neurons and modulatory monoaminergic neurons. Is such biochemical diversity also correlated with clonal units? GABAergic and monoaminergic neurons in the mammalian brain are mostly formed in distinct subregions and therefore belong to specific cell lineages [33–35]. Similarly, GABAergic projection neurons and glutamatergic local neurons in the insect AL are formed by specialized clones [36, 37]. We therefore asked whether the formation of neurons with particular transmitters would be closely correlated with clonal units.

We coregistered the brain labeled with anti-GABA antibody with those of the clones. Considering that locations of clonal cell bodies may fluctuate slightly between individuals, we

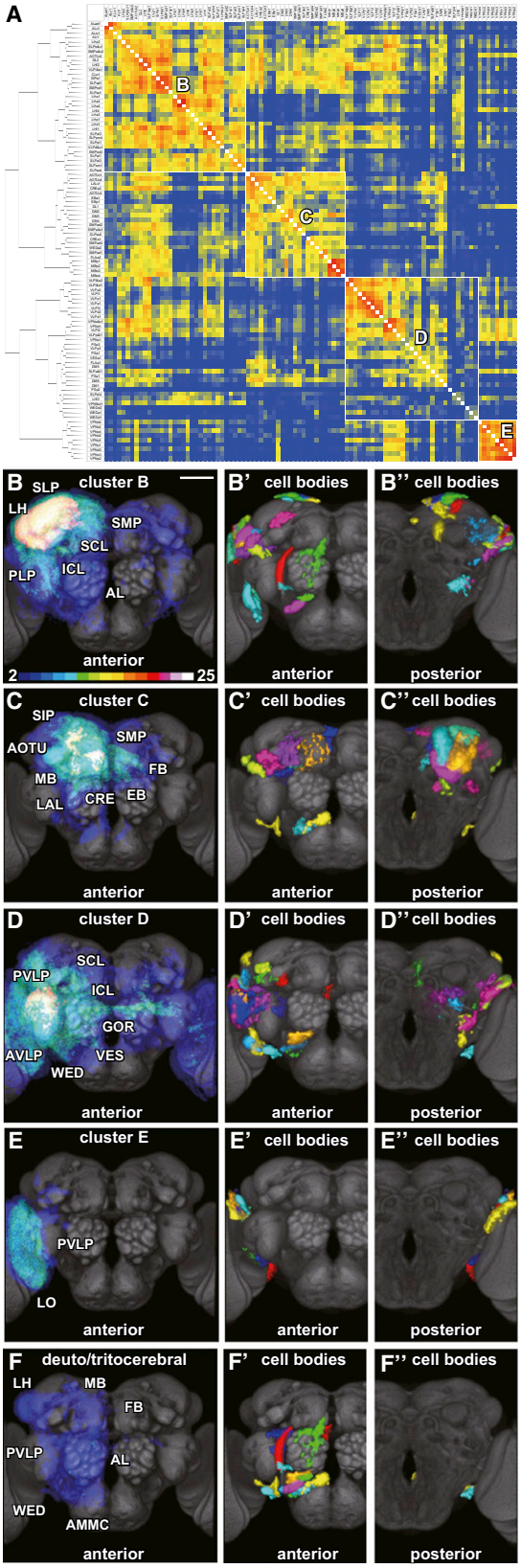

Figure 4. Overlap between Clonal Arborizations

(A) Cluster analysis of the clones with spatial overlap. Color code denotes the number of overlapping voxels between each combination of clones.

(B–E) Boxes framed in white show the four clusters of clones with high spatial overlap. A larger image of the diagram is provided in Figure S4. In (B)–(E), overlay images of the clones that form the four clusters indicated in (A) are seen. Leftmost panels show the overlay of arborizations. Color code denotes the number of overlapping clones. Middle (′) and right (″) panels show the distribution of cell bodies of these clones (shown in different colors) in the anterior (middle, ′) and posterior (right, ″) brains.

(F) Overlay images of putative deuto- and tritocerebral clones. Scale bar represents 50 μm.

identified clones that are likely to contain GABAergic neurons only when the labeled cell locations were within the possible fluctuation level and found at least 45 such clones (Table 1A). Characteristic cell positions and projection patterns labeled with the anti-5-hydroxytryptamine (5HT), tyrosine hydroxylase (TH), and tyrosine decarboxylase 2 (TDC2) antibodies enabled us to identify seven, eight, and eight clones that produce serotonin, dopamine, and octopamine, respectively (Table 1A).

In most cases the number of the GABAergic or monoaminergic cells was smaller than the average cell number of the clones that occupy that location, and the projections of monoaminergic cells cover only subsets of the entire projections of the associated clones. Registration of GABAergic or monoaminergic neurons with clonal cell clusters suggests that they may coexist in a single clone (Figure S5). These findings indicate that neurons with multiple types of transmitters are generated in many, if not all, of the clones.

In the vertebrate brain, monoaminergic neurons form extensive projections, whereas GABAergic neurons are mostly local interneurons. Consistent with this, all but one of the clones featuring monoaminergic neurons have extensive projections (Table 1B). In contrast, only half of the locally arborizing clones contain GABAergic cells.

Community Analysis of Neural Projections

The comprehensive collection of clones serves as a useful tool for providing a systematic view of the entire set of neural projections in the brain, the projectome [38]. As discussed earlier, a clonal unit may contain several neuronal subgroups with different projection patterns. By tracing the fiber bundles arising from the cell-body clusters, we identified in total 247 such projection subgroups (Table S5). Although single neurons in each subgroup may further show variability in their fine projection patterns, analysis of these subgroups should provide an acceptable overview of the existing neural network.

Using these data, we first made a connection map of the cerebrum (Figure 5A). The map evaluates the clonal variety of connections rather than the actual number of neurons connecting them. Neuropils like the SMP, SLP, SCL, and ICL have a large number of connections with others, serving as the hubs, whereas those of the AL, MB, and CX have many fewer connections. This is consistent with the differences in the number of clones that arborize in them (Figures 3R–3V). The number of bilateral connections was highly variable between neuropils (Figure 5B), with abundant connections in, e.g., SMP, superior intermediate protocerebrum (SIP), SLP, SCL, ICL, SPS, and AVLP but none in, e.g., MB calyx and LH.

The network is characterized by a small average distance between pairs of neuropils and an abundance of mutually connected triplets of neuropils. This indicates that the network has the so-called small-world property, meaning that most nodes in the network can be reached from all other nodes by a small number of connections [39, 40] (see Supplemental Discussion for detail). The node degree (*k*, number of neuropils connected to a given neuropil, Figure S6A and Table S4) and node

Please cite this article in press as: Ito et al., Systematic Analysis of Neural Projections Reveals Clonal Composition of the *Drosophila* Brain, Current Biology (2013), http://dx.doi.org/10.1016/j.cub.2013.03.015

Table 1. Correlation between Clones and Transmitters

A

Clone	GABA	Serotonin	Dopamine	Octopamine	Arbor
ALad1	■				P
ALl1	■				P
ALlv1	■				P
ALv1	■				P
AOTUv1	■				P
AOTUv2	■				P
AOTUv3		■			P
AOTUv4					P
CLp1					L
CREa1	■		■	■	P
CREa2	■		■	■	P
DL1	■		■		P
DL2			■		P
DM1	■			■	P
DM2	■				P
DM3	■	■		■	P
DM4	■	■	■		P
DM5	■	■	■		P
DM6			■		P
EBa1	■	■			P
EBp1			■		P
FLAa1					P
FLAa2	■				P
LALv1	■				P
LHa1	■				L
LHa2	■				L
LHa3	■				L
LHa4					L
LHd1			■		P
LHl1	■				L
LHl2	■				P
LHl3					P
LHl4	■				P
LHp1					L
LHp2	■				P
MBp1					P
MBp2					P
MBp3					P
MBp4					P
PSa1	■			■	P
PSp1					P
PSp2					P
PSp3					P
SIPa1	■				L
SLPa&l1	■				P
SLPad1					P
SLPal1					L
SLPal2	■				L
SLPal3	■				P
SLPav1					P
SLPav2	■				P
SLPav4					L
SLPp&v1	■				P
SLPpl1					P
SLPpl4					L
SLPpm1					P
SLPpm4					L
SMPad1					P
SMPad2					P
SMPad4	■			■	P
SMPp&v1	■	■			P
SMPp&v2	■				P
SMPpd1					P
SMPpd2					P
VESa1	■				P
VLPa1					L
VLPa2					P
VLPd&p1					P
VLPd1					P
VLPd2					P
VLPl&d1	■				P
VLPl&p1					P
VLPl&p2	■				P
VLPl1	■				L
VLPl2	■				P
VLPl3					L
VLPp&l1	■				P
VLPp1		■			L
VLPp2					P
VPNd1	■				P
VPNd2					P
VPNd3					P
VPNd4	■				P
VPNl&d1	■	■			P
VPNp&v1	■				P
VPNp1					P
VPNp2					P
VPNp3					P
VPNp4					P
VPNv1	■				P
VPNv2					P
VPNv3					P
WEDa1	■				L
WEDa2	■				L
WEDd1					P
WEDd2	■				P

B

	GABA	Serotonin	Dopamine	Octopamine
Local	9	1	0	0
Projection	36	6	8	7

(A) Clones that contain neurons with GABA, serotonin, dopamine, and octopamine transmitters. Gray and black boxes indicate that a small or large, respectively, subset of the neurons in the clonal cell cluster are labeled to feature these transmitters. Letters "P" and "L" in the "Arbor" column indicate whether the clone has only local arborizations (L) or contains projection neurons (P). See also Figure S5.

(B) Correlation between transmitters and arborization types of the clones.

strength (*s*, number of projection subgroups that mediate these connections, shown by the reddish hue in Figure 5A) are both bimodally distributed. *s* superlineally depends on *k* (Figure 5C), indicating that a neuropil connected to many other neuropils (i.e., large *k*) tends to be connected to each of them by a large clonal variety of connections (i.e., large *s*/*k*). Although the dependence of *s* on *k* has not been systematically investigated for brain networks, such superlinear dependence is commonly observed in various types of networks [41].

To further reveal global organization of the connection map, we carried out a community analysis, i.e., partitioning the network into densely connected communities. Because synaptic contacts between neurons of different clones cannot be assumed safely at the current state of our knowledge, we examined only direct connections between neuropils via each projection subgroup, without assuming any interneuronal contacts. Considering the abundance of neurons that also contribute to the network of contralateral neuropils, we took into account the 494 projection subgroups of both brain sides.

Blondel's algorithm for community detection [42] identified five communities (white boxes 1–5 in Figure 5D). The *Q* value ($0 \leq Q \leq 1$, a factor to quantify the quality of the obtained partitioning) was 0.301, suggesting mild community structure of the network. Communities 1–3 contain neuropils of the ventral, dorsal-lateral, and dorsal-medial cerebrum, respectively, and communities 4 and 5 correspond to the right and left MBs (Figures 5H–5L). Though communities 1–3 contain corresponding neuropils of both brain sides, the pair of MBs is separated into distinct communities (4 and 5) because of the few commissural connections between them.

To assess the extent of inter- and intracommunity communication, for each neuropil we calculated the node strength originating from the neuropils of different communities and those within the same community (extrinsic and intrinsic node strengths, s_{ex} and s_{in}). Although s_{ex} and s_{in} are highly correlated for communities 1 and 2 ($R^2 > 0.70$) (Figures S6G–S6L), community 3 has two subpopulations with high and low s_{ex}/s_{in} ratios. Interestingly, the latter subpopulation of community 3 exactly matches with the neuropils of the CX (yellow box in Figure 5D), suggesting their limited intercommunity communication. Communities 4 and 5 (right and left MBs) also possess low s_{ex}/s_{in} ratios. Indeed, the links incident to the CX neuropils are mostly confined within community 3, and the MBs have only a limited amount of intercommunity links (Figure 5D). Thus, in spite of their importance in higher-order brain functions, the CX and MB are relatively isolated structures in the fly brain, communicating with only specific neuropils.

Discussion

Through extensive clonal identification and comparison, we show here that the basic concept of the clonal units—that the progeny of a single neuroblast form distinct structural subtypes of neurons that contribute to specific parts of the insect brain [7, 10]—is broadly applicable to all the neuroblast lineages. Many clones are heterogeneous both in terms of projection patterns and biochemical transmitter properties. Gene expression patterns are also heterogeneous, as has been shown in the clusters of *fruitless*-expressing cells scattered in numerous clones [16]. Neuropils are composed synergistically of multiple clones. The degree of clonal overlap varies greatly depending on neuropils. The entire brain neural network consists of several neuropil communities connected with varying degrees of clonal projections. Fiber bundles are also organized clonally. Asymmetric distributions of presynaptic sites showed that clonal units propagate information not only from proximal to distal but also in the opposite direction in various cases. Analysis of clonal units thus provides an overarching view of the organized architecture of brain neuropils as well as crucial aspects of what cell arrangements characterize a neural network.

Clonal Organization of the Structurally and Functionally Heterogeneous Neural Populations

Considering the vast number of identified clones with specific cell-body locations and projection patterns, most clonal units in the fly cerebrum should be unique. In a few cases, indistinguishable clonal units might be generated redundantly

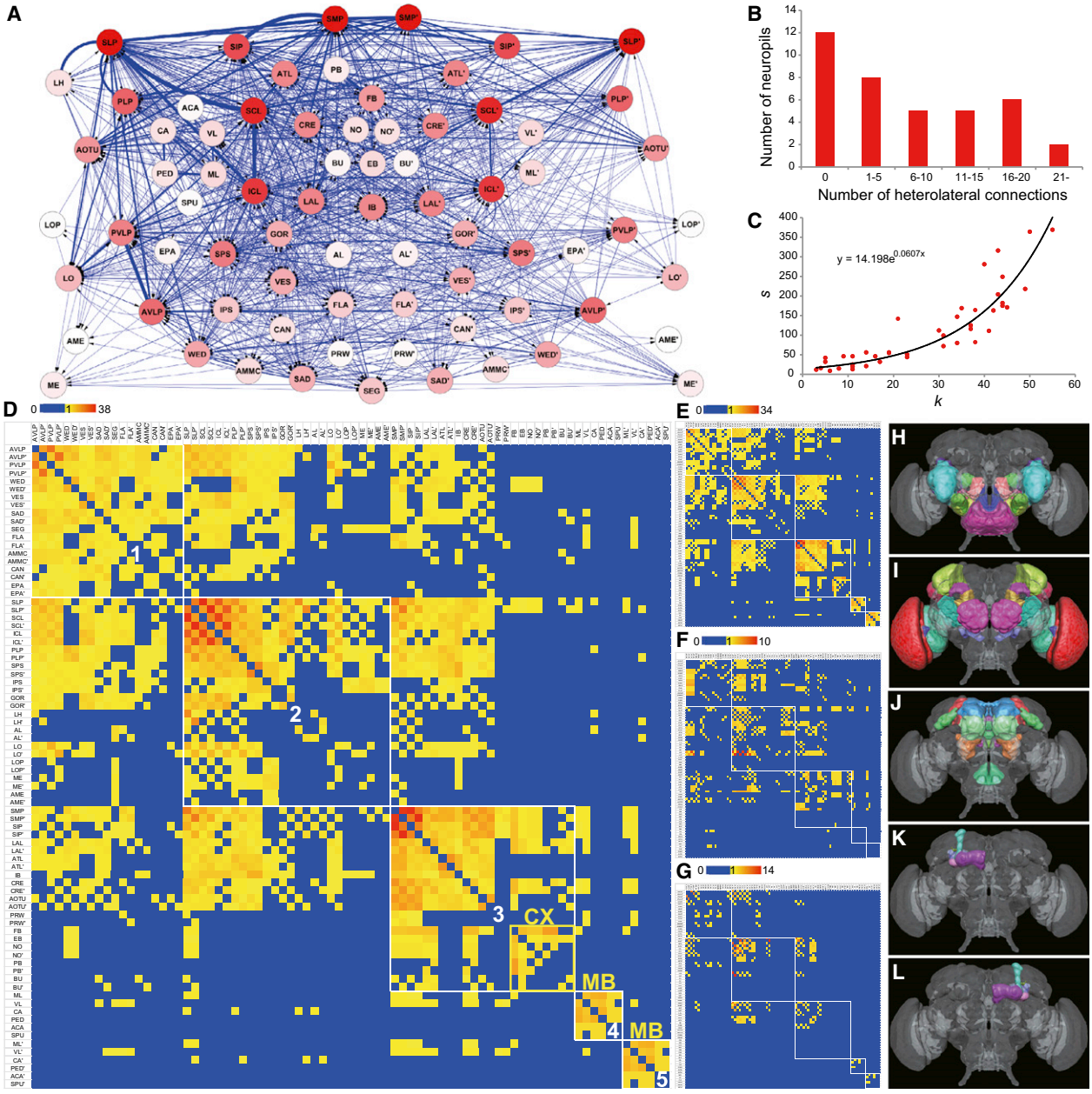

Figure 5. Network Analysis of the Clonal Projections

(A) Network diagram of the connections between neuropils. Neuropil names with apostrophe (′) indicate those in the contralateral brain side. Thickness of the lines indicates the number of projection subgroups that contribute to the link between two neuropils. Reddish hue at each neuropil indicates the total number of connections associated with it. Arrows indicate the estimated direction of information, polarizing the direction from the arborization lacking presynaptic sites to that with presynaptic sites. Neuropils in the ventral cerebrum have fewer connections than in the dorsal cerebrum, in part because connections made by the clones in the SEG were not analyzed in the current study.

(B) Number of bilateral connections for each neuropil.

(C) Scatter diagram of node degree (*k*, number of neuropils directly connected to a given neuropil) and node strength (*s*, number of projection subgroups that mediate these connections).

(D) Matrix diagram of connections between neuropils. Color code represents the number of clonal connections. White frames indicate the five communities of closely associated neuropils. Yellow frame indicates the neuropils that comprise the CX.

(E–G) Connections mediated by specific types of clonal arborizations. Connections of projection neurons without asymmetric distribution of presynaptic sites are shown in (E). Connections of projection neurons with asymmetric presynaptic sites are shown in (F). Rows denoted along the ordinates (left sides) indicate the input neuropils lacking presynaptic sites; rows denoted along the top of the diagram indicate the output neuropils with presynaptic sites. Such connections are found from the optic lobe to the cerebrum, from lower auditory centers to AVLP and PVLP, from the anterior ventral cerebrum to the VLP and SCL/ICL, from dorsal cerebrum to the CX and MB lobes, from the FB to dorsal and ventral cerebrum, and from the IB to various neuropils. Connections mediated by locally arborizing clones are shown in (G). Larger images of diagrams in (A) and (D)–(G) are provided in Figure S6.

(H–L) The five groups of neuropils indicated in (D), anterior view.

by more than one neuroblast. The wide variance in clone-induction frequency among neuroblasts made it difficult to assess the existence of such redundancy. However, even the four nearly identical MB clones [7] are actually unique, in that each clone arborizes in characteristic subregions of the calyx [10] and that early embryonic neurons show lineage-specific projections [43], supporting the idea of the uniqueness of most clones. Neuroblasts in the embryonic brain are uniquely identifiable by the combination of genes they express [12], suggesting that the clonal identity should directly be correlated with the neuroblast identity.

As discussed previously [10], neuronal variety in a clone can be determined by two factors: birth order of neurons and fate determination between sibling neurons. Different types of neurons are generated sequentially in a time-dependent manner, as has been reported for the AL and MB [9, 44]. Neuroblasts change their gene expression patterns drastically during neurogenesis [45], some of which control the generation of specific cell types [46]. The GMCs generated by the neuroblasts divide once more to give rise to sibling neurons with high and low Notch activities, forming two lines of hemilineages [47]. Chromatin modification observed in the Notch-mediated fate determination of peripheral olfactory sensory neurons [48] might also work in the hemilineages of clonal units.

Structural Properties of the *Drosophila* Brain Network

The network of the *Drosophila* brain obtained in this study has the small-world property, heterogeneous distributions of the node degree (k) and node strength (s), and community structure. These are consistent with the properties of the structural and functional brain networks of mammals, including humans [40], as well as those of the *C. elegans* neural network [39, 49, 50].

The detected communities show an interesting functional correlation with sensory pathways. The three major secondary visual centers (PVLP, PLP, and AOTU) are separated in communities 1, 2, and 3, respectively, because they are connected with other neuropils with rather different preferences. The neuropils having extensive connections with the primary auditory center (AMMC) are all categorized in community 1. In the olfactory system, the AL/LH, MB, and the so-called MB-associated neuropils (SMP, SIP, and CRE), which feature extensive connections with the MB lobes [25], are categorized into different communities (2, 4 and 5, and 3, respectively) because of the limited variety of connections of the MB and differently preferential connections of the AL/LH and MB-associated neuropils with other neuropils. These data suggest that the visual information sent to the three secondary centers would be processed in different ways, among which is that information sent to community 1 is most likely to be integrated with the auditory information and information sent to communities 2 and 3 would be integrated with different types of olfactory information.

These results were not consistent with the cluster analysis based on randomly labeled single neurons by Chiang et al. [18], which categorized all the visual centers and olfactory centers into single groups. This is because our analysis is more sensitive to the different varieties of connections between neuropils than to the number of parallel fibers connecting the primary and secondary sensory centers of each modality (see Supplemental Discussion).

Connections between neuropils can be categorized into three types. First, 67% of connections are mediated by the projection neurons with no apparent asymmetric distribution of presynaptic sites (Figure 5E). These may mediate bidirectional or unidirectional communication, depending on the asymmetric distribution of postsynaptic sites, which we did not analyze because of technical complexity. Second, 26% of connections showed presynaptic sites only at one end, which should play important roles in the directed information flow (Figure 5F). And third, the remaining 7% of connections are mediated by local arborizations spanning neighboring neuropils (Figure 5G). They contribute only to specific connections, notably between communities 1 and 2 as well as 2 and 3, but hardly between communities 1 and 3.

Clonal Units across Species

Studies in other insects also revealed similar clonally organized structures in the brain [8], suggesting that the clonal units should be evolutionarily conserved organizations across the Insecta. The number of stem cells is rather similar between diverse species, like locusts and flies [51], suggesting the existence of a similar variety of clonal units. Identification of clonal units in other insects, especially in their diffuse neuropils, should provide an organized view about the consensus structure of the insect brain.

Mammalian excitatory and inhibitory neurons are mostly made by different stem cells [34], with a few reported exceptions [52], whereas many *Drosophila* stem cells produce neurons with different transmitters. Recent clonal studies in the mammalian cortex show, however, important similarities between mammals and insects. Specific visual characteristics are processed by the clonally associated neurons in the mammalian visual cortex [5, 6] and clonally organized layers in the fly FB [30]. Neuronal and glial lineages are mixed in the mammalian brain [53], and at least some *Drosophila* lineages produce both neurons and glia [21, 54]. As in the fly brain, a clone in the mammalian cortex contains a variety of neural types that are generated sequentially during neurogenesis [3]. Although many insect neurons do not migrate, whereas mammalian neurons migrate extensively, the former neurons form dendritic arborization not in their cell bodies but in distant parts of their neurites. Thus, both in mammals and insects, dendrites of clonally associated neurons may often be detached from their birthplace.

Evolutionary clades leading to mammals and insects diverged more than 550 million years ago, and the mammalian neocortex is a recent structure that is absent in other vertebrates. Analysis of clonal organization in more conventional regions of the mammalian brain may reveal further similarities across species.

Conclusions

Identification of most of the clonally associated units in the *Drosophila* brain revealed organized architecture both in the well-known and hardly investigated neuropils. Because of the relatively small number of units to be analyzed and their importance in developmental and evolutionary aspects, understanding the brain from the clonal point of view should be an efficient way to reveal its neural network architecture.

Experimental Procedures

Fly Strains and Clone Labeling

The following genetic cross and heat-shock conditions were used to label clones: *elav^{c155}-Gal4 hs-FLP*; *FRT^{G13} tub-GAL80* crossed with *UAS-DsRed*; *FRT^{G13}*; *UAS-n-Syb::GFP* (heat shock at 36°C for 45 min); *elav^{c155}-Gal4*

hs-FLP; FRT^{G13} *tub-GAL80* crossed with *UAS-Syt::HA*; FRT^{G13} *UAS-GFP*; *UAS-mCD8::GFP* (36°C for 45 min); *hs-FLP tub-GAL80* FRT^{19A}; *actin-Gal4* crossed with *UAS-DsRed* FRT^{19A}; +; *UAS-n-Syb::GFP* (36°C for 30 min); *hs-FLP tub-GAL80* FRT^{19A}; *actin-Gal4* crossed with FRT^{19A}; *UAS-GFP* (37°C for 30 min). In all cases, heat shock was applied between 12–36 hr after egg laying. Heat-shock conditions were adjusted so that progeny of one or only a few neuroblasts would be labeled in a brain sample. To label dopaminergic cells for registration, *TH-GAL4* strain was crossed with *UAS-mCD8::GFP* strain.

Sample Preparation

Flies were raised at 25°C with a 12 h/12 h light/dark cycle, and female flies were examined between 4 and 10 days after eclosion. Brains were dissected and labeled with antibody as previously described [28]. The following primary antibodies were used: rabbit anti-DsRed antibody (Takara Bio; #632496, 1:1,000), rat anti-GFP (Nacalai Tesque; #GF090R, 1:1,000), rabbit anti-GFP (Molecular Probe; #A11122, 1:1,000), rat anti-HA (Roche; #11 867 423 001, 1:500), mouse nc82 (gift from E. Buchner and A. Hofbauer, 1:20), rabbit anti-GABA (Sigma-Aldrich; A2052, 1:1,000), rabbit anti-5HT (DiaSorin; 20080, lot 051007, 1:2,000), mouse anti-TH (ImmunoStar; #907001, 1:500), and rabbit anti-TDC2 (Abcam, #GR84243-2, 1:1,000).

Image Processing

Confocal image stacks were acquired by Zeiss LSM 510 confocal microscopes at 1024 × 1024 pixel resolution every 1.28 μm (0.32 × 0.32 × 1.28 μm), using water-immersion 40× Plan-Apochromat objectives (numerical aperture = 1.2). For the samples with relatively weak labeling, noise was suppressed using 3D deconvolution software cellSens Dimension (Olympus). Image stacks were imported to 3D modeling software Amira 5.2.2 (Mercury). Signals of cell-body clusters, bundles of neural fibers, and clonal unit arborization areas were manually selected in each layer. Signals of unselected regions, including background noise and signals of other neurons, were erased using a macro program of ImageJ (NIH). Cleaned image stacks were registered using brain aligner [22] or registration plugin in Fiji [23] to the standard brain template presented in Cachero et al. [16]. Three-dimensional reconstruction images were produced with FluoRender [55].

Detection of Network Communities

We used Blondel's algorithm adopted for weighted networks [42] because it provides partitioning with larger *Q* values than other algorithms for various types of networks [42, 56]. *Q* values, also called modularity, are calculated by a combination of a given network and the partitioning result [56, 57]. *Q* values larger than 0.3 suggest that the given network has community structure [57].

Supplemental Information

Supplemental Information includes Supplemental Discussion, Supplemental Experimental Procedures, six figures, five tables, and one movie and can be found with this article online at http://dx.doi.org/10.1016/j.cub.2013.03.015.

Acknowledgments

We are grateful to N. Strausfeld and K. Hanashima for discussion. We thank T. Awasaki and T. Lee for communicating results prior to publication; B. Dickson, M. Ramaswami, and the Bloomington Drosophila Stock Center for fly strains; J. Tanimura for sharing antibody-labeling data; and S. Shuto, K. Yamashita, and H. Hirose for technical assistance. This work was supported by a CREST/JST grant to K.I. and Grant-in-Aid for Scientific Research from the Ministry of Education, Culture, Sports, Science and Technology of Japan to K.I. and N.M. The transgenic animal experiments are approved by the review board of IMCB.

Received: October 15, 2012
Revised: January 30, 2013
Accepted: March 4, 2013
Published: March 28, 2013

References

1. Ramon y Cajal, S. (1909). Histology of the Nervous System of Man and Vertebrates (New York: Oxford University Press).
2. Sawa, H. (2010). Specification of neurons through asymmetric cell divisions. Curr. Opin. Neurobiol. *20*, 44–49.
3. Molyneaux, B.J., Arlotta, P., Menezes, J.R., and Macklis, J.D. (2007). Neuronal subtype specification in the cerebral cortex. Nat. Rev. Neurosci. *8*, 427–437.
4. Costa, M.R., and Hedin-Pereira, C. (2010). Does cell lineage in the developing cerebral cortex contribute to its columnar organization? Front Neuroanat *4*, 26.
5. Ohtsuki, G., Nishiyama, M., Yoshida, T., Murakami, T., Histed, M., Lois, C., and Ohki, K. (2012). Similarity of visual selectivity among clonally related neurons in visual cortex. Neuron *75*, 65–72.
6. Li, Y., Lu, H., Cheng, P.L., Ge, S., Xu, H., Shi, S.H., and Dan, Y. (2012). Clonally related visual cortical neurons show similar stimulus feature selectivity. Nature *486*, 118–121.
7. Ito, K., Awano, W., Suzuki, K., Hiromi, Y., and Yamamoto, D. (1997). The *Drosophila* mushroom body is a quadruple structure of clonal units each of which contains a virtually identical set of neurones and glial cells. Development *124*, 761–771.
8. Boyan, G., and Williams, L. (2011). Embryonic development of the insect central complex: insights from lineages in the grasshopper and *Drosophila*. Arthropod Struct. Dev. *40*, 334–348.
9. Lai, S.L., Awasaki, T., Ito, K., and Lee, T. (2008). Clonal analysis of *Drosophila* antennal lobe neurons: diverse neuronal architectures in the lateral neuroblast lineage. Development *135*, 2883–2893.
10. Ito, K., and Awasaki, T. (2008). Clonal unit architecture of the adult fly brain. Adv. Exp. Med. Biol. *628*, 137–158.
11. Ito, K., and Hotta, Y. (1992). Proliferation pattern of postembryonic neuroblasts in the brain of *Drosophila melanogaster*. Dev. Biol. *149*, 134–148.
12. Urbach, R., and Technau, G.M. (2003). Molecular markers for identified neuroblasts in the developing brain of *Drosophila*. Development *130*, 3621–3637.
13. Prokop, A., and Technau, G.M. (1991). The origin of postembryonic neuroblasts in the ventral nerve cord of *Drosophila melanogaster*. Development *111*, 79–88.
14. Bello, B.C., Izergina, N., Caussinus, E., and Reichert, H. (2008). Amplification of neural stem cell proliferation by intermediate progenitor cells in *Drosophila* brain development. Neural Dev. *3*, 5.
15. Boone, J.Q., and Doe, C.Q. (2008). Identification of *Drosophila* type II neuroblast lineages containing transit amplifying ganglion mother cells. Dev. Neurobiol. *68*, 1185–1195.
16. Cachero, S., Ostrovsky, A.D., Yu, J.Y., Dickson, B.J., and Jefferis, G.S. (2010). Sexual dimorphism in the fly brain. Curr. Biol. *20*, 1589–1601.
17. Yu, J.Y., Kanai, M.I., Demir, E., Jefferis, G.S., and Dickson, B.J. (2010). Cellular organization of the neural circuit that drives *Drosophila* courtship behavior. Curr. Biol. *20*, 1602–1614.
18. Chiang, A.S., Lin, C.Y., Chuang, C.C., Chang, H.M., Hsieh, C.H., Yeh, C.W., Shih, C.T., Wu, J.J., Wang, G.T., Chen, Y.C., et al. (2011). Three-dimensional reconstruction of brain-wide wiring networks in *Drosophila* at single-cell resolution. Curr. Biol. *21*, 1–11.
19. Hampel, S., Chung, P., McKellar, C.E., Hall, D., Looger, L.L., and Simpson, J.H. (2011). *Drosophila* Brainbow: a recombinase-based fluorescence labeling technique to subdivide neural expression patterns. Nat. Methods *8*, 253–259.
20. Lee, T., and Luo, L. (1999). Mosaic analysis with a repressible cell marker for studies of gene function in neuronal morphogenesis. Neuron *22*, 451–461.
21. Yu, H.-H., Awasaki, T., Schroeder, M.D., Long, F., Yang, J.S., He, Y., Ding, P., Kao, J.-C., Jenett, A., Wu, G.Y.-Y., et al. (2013). Clonal development and organization of the adult Drosophila central brain. Curr.Biol. Published online March 28, 2013. http://dx.doi.org/10.1016/j.cub.2013.02.057.
22. Peng, H., Chung, P., Long, F., Qu, L., Jenett, A., Seeds, A.M., Myers, E.W., and Simpson, J.H. (2011). BrainAligner: 3D registration atlases of *Drosophila* brains. Nat. Methods *8*, 493–500.
23. Schindelin, J., Arganda-Carreras, I., Frise, E., Kaynig, V., Longair, M., Pietzsch, T., Preibisch, S., Rueden, C., Saalfeld, S., Schmid, B., et al. (2012). Fiji: an open-source platform for biological-image analysis. Nat. Methods *9*, 676–682.
24. Izergina, N., Balmer, J., Bello, B., and Reichert, H. (2009). Postembryonic development of transit amplifying neuroblast lineages in the *Drosophila* brain. Neural Dev. *4*, 44.
25. Tanaka, N.K., Tanimoto, H., and Ito, K. (2008). Neuronal assemblies of the *Drosophila* mushroom body. J. Comp. Neurol. *508*, 711–755.

26. Otsuna, H., and Ito, K. (2006). Systematic analysis of the visual projection neurons of *Drosophila melanogaster*. I. Lobula-specific pathways. J. Comp. Neurol. *497*, 928–958.
27. Kamikouchi, A., Shimada, T., and Ito, K. (2006). Comprehensive classification of the auditory sensory projections in the brain of the fruit fly *Drosophila melanogaster*. J. Comp. Neurol. *499*, 317–356.
28. Miyazaki, T., and Ito, K. (2010). Neural architecture of the primary gustatory center of *Drosophila melanogaster* visualized with GAL4 and LexA enhancer-trap systems. J. Comp. Neurol. *518*, 4147–4181.
29. Hanesch, U., Fischbach, K.-F., and Heisenberg, M. (1989). Neuronal architecture of the central complex in *Drosophila melanogaster*. Cell Tissue Res. *257*, 343–366.
30. Liu, G., Seiler, H., Wen, A., Zars, T., Ito, K., Wolf, R., Heisenberg, M., and Liu, L. (2006). Distinct memory traces for two visual features in the *Drosophila* brain. Nature *439*, 551–556.
31. Mu, L., Ito, K., Bacon, J.P., and Strausfeld, N.J. (2012). Optic glomeruli and their inputs in *Drosophila* share an organizational ground pattern with the antennal lobes. J. Neurosci. *32*, 6061–6071.
32. Strausfeld, N.J. (2012). Arthropod Brains: Evolution, Functional Elegance, and Historical Significance (Cambridge, MA: Harvard University Press).
33. McKay, R. (1997). Stem cells in the central nervous system. Science *276*, 66–71.
34. Brown, K.N., Chen, S., Han, Z., Lu, C.H., Tan, X., Zhang, X.J., Ding, L., Lopez-Cruz, A., Saur, D., Anderson, S.A., et al. (2011). Clonal production and organization of inhibitory interneurons in the neocortex. Science *334*, 480–486.
35. Bonilla, S., Hall, A.C., Pinto, L., Attardo, A., Götz, M., Huttner, W.B., and Arenas, E. (2008). Identification of midbrain floor plate radial glia-like cells as dopaminergic progenitors. Glia *56*, 809–820.
36. Okada, R., Awasaki, T., and Ito, K. (2009). Gamma-aminobutyric acid (GABA)-mediated neural connections in the *Drosophila* antennal lobe. J. Comp. Neurol. *514*, 74–91.
37. Das, A., Chiang, A., Davla, S., Priya, R., Reichert, H., Vijayraghavan, K., and Rodrigues, V. (2011). Identification and analysis of a glutamatergic local interneuron lineage in the adult *Drosophila* olfactory system. Neural Syst Circuits *1*, 4.
38. Kasthuri, N., and Lichtman, J.W. (2007). The rise of the 'projectome'. Nat. Methods *4*, 307–308.
39. Watts, D.J., and Strogatz, S.H. (1998). Collective dynamics of 'small-world' networks. Nature *393*, 440–442.
40. Bullmore, E., and Sporns, O. (2009). Complex brain networks: graph theoretical analysis of structural and functional systems. Nat. Rev. Neurosci. *10*, 186–198.
41. Barrat, A., Barthélemy, M., Pastor-Satorras, R., and Vespignani, A. (2004). The architecture of complex weighted networks. Proc. Natl. Acad. Sci. USA *101*, 3747–3752.
42. Blondel, V.D., Guillaume, J.-L., Lambiotte, R., and Lefebvre, E. (2008). Fast unfolding of communities in large networks. J. Stat. Mech. *2008*, P10008.
43. Kunz, T., Kraft, K.F., Technau, G.M., and Urbach, R. (2012). Origin of *Drosophila* mushroom body neuroblasts and generation of divergent embryonic lineages. Development *139*, 2510–2522.
44. Lee, T., Lee, A., and Luo, L. (1999). Development of the *Drosophila* mushroom bodies: sequential generation of three distinct types of neurons from a neuroblast. Development *126*, 4065–4076.
45. Isshiki, T., Pearson, B., Holbrook, S., and Doe, C.Q. (2001). *Drosophila* neuroblasts sequentially express transcription factors which specify the temporal identity of their neuronal progeny. Cell *106*, 511–521.
46. Doe, C.Q. (2006). Chinmo and neuroblast temporal identity. Cell *127*, 254–256.
47. Truman, J.W., Moats, W., Altman, J., Marin, E.C., and Williams, D.W. (2010). Role of Notch signaling in establishing the hemilineages of secondary neurons in *Drosophila melanogaster*. Development *137*, 53–61.
48. Endo, K., Karim, M.R., Taniguchi, H., Krejci, A., Kinameri, E., Siebert, M., Ito, K., Bray, S.J., and Moore, A.W. (2012). Chromatin modification of Notch targets in olfactory receptor neuron diversification. Nat. Neurosci. *15*, 224–233.
49. Sohn, Y., Choi, M.-K., Ahn, Y.-Y., Lee, J., and Jeong, J. (2011). Topological cluster analysis reveals the systemic organization of the *Caenorhabditis elegans* connectome. PLoS Comput. Biol. *7*, e1001139.
50. Pan, R.K., Chatterjee, N., and Sinha, S. (2010). Mesoscopic organization reveals the constraints governing *Caenorhabditis elegans* nervous system. PLoS ONE *5*, e9240.
51. Broadus, J., and Doe, C.Q. (1995). Evolution of neuroblast identity: *seven-up* and *prospero* expression reveal homologous and divergent neuroblast fates in *Drosophila* and *Schistocerca*. Development *121*, 3989–3996.
52. Letinic, K., Zoncu, R., and Rakic, P. (2002). Origin of GABAergic neurons in the human neocortex. Nature *417*, 645–649.
53. Alvarez-Buylla, A., García-Verdugo, J.M., and Tramontin, A.D. (2001). A unified hypothesis on the lineage of neural stem cells. Nat. Rev. Neurosci. *2*, 287–293.
54. Bossing, T., Udolph, G., Doe, C.Q., and Technau, G.M. (1996). The embryonic central nervous system lineages of *Drosophila melanogaster*. I. Neuroblast lineages derived from the ventral half of the neuroectoderm. Dev. Biol. *179*, 41–64.
55. Wan, Y., Otsuna, H., Chien, C.-B., and Hansen, C. (2009). An interactive visualization tool for multi-channel confocal microscopy data in neurobiology research. IEEE Trans. Vis. Comput. Graph. *15*, 1489–1496.
56. Fortunato, S. (2010). Community detection in graphs. Phys. Rep. *486*, 75–174.
57. Newman, M.E.J., and Girvan, M. (2004). Finding and evaluating community structure in networks. Phys. Rev. E Stat. Nonlin. Soft Matter Phys. *69*, 026113.